Original Article

Reversal of diabetes in NOD mice by clinical-grade pro-insulin and IL10 secreting *Lactococcus lactis* in combination with low-dose anti-CD3 depends on the induction of Foxp3-positive T cells

Running title: Tregs sustain disease reversal by *L. lactis* therapy

T. Takiishi [1,a,b], D. P. Cook [1,b], H. Korf [1], G. Sebastiani [2], F. Mancarella[2], J.P.M.C.M. Cunha[1], C. Wasserfall [3], N. Casares[4], J.J. Lasarte[4], L. Steidler [5], P. Rottiers [5], F. Dotta [2], C. Gysemans [1,c], C. Mathieu [1,c]

[1]Laboratory of Clinical and Experimental Endocrinology (CEE), Campus Gasthuisberg O&N1, Katholieke Universiteit Leuven (KU LEUVEN), Leuven, Belgium. [2]Diabetes Unit, Department of Internal Medicine, Endocrine and Metabolic Sciences and Biochemistry, University of Siena and Fondazione Umberto Di Mario ONLUS – Toscana Life Science Park, Siena, Italy. [3]UF Department of Pathology, Immunology and Laboratory Medicine, College of Medicine, Gainesville, Florida. [4]Immunology and Immunotherapy Program, Center for Applied Medical Research (CIMA), University of Navarra, Pamplona, Spain. [5]Intrexon ActoBiotics NV, Zwijnaarde (Ghent), Belgium.

[a]current address: Instituto de Ciências Biomédicas. Universidade de São Paulo (USP), São Paulo, Brazil. [b]T.T and D.P.C share first authorship; [c]C.G. and C.M. share senior authorship.

Corresponding author: Conny Gysemans, Katholieke Universiteit Leuven (KU LEUVEN), Campus Gasthuisberg O&N1, Laboratory of Clinical and Experimental Endocrinology (CEE), Herestraat 49 box 902, 3000 Leuven, Belgium. TEL: +32 16 377454; FAX: +32 16 330728. Email: conny.gysemans@kuleuven.be

Character count: abstract (200 words); body (3858 words); figures (7); tables (0)

Introduction of beta cell auto-antigens via the gut through *Lactococcus lactis (L. lactis)* has been demonstrated to be a promising approach for diabetes reversal in NOD mice. Here we show that a combination of low-dose anti-CD3 with a clinical-grade self-containing *L. lactis* appropriate for human application secreting human pro-insulin and IL10 cured 66% of new-onset diabetic mice, comparable to plasmid-driven *L. lactis*. Initial blood glucose concentrations (<350 mg/dl) and insulin autoantibody positivity were predictors of stable reversal of hyperglycemia and decline in IAA positivity was an immune biomarker of therapeutic outcome. Assessment of the immune changes induced by the *L. lactis*-based therapy revealed elevated frequencies of $CD4^+Foxp3^+$ T cells in the pancreatic draining lymph nodes, pancreas, and peripheral blood of all treated mice, independent of metabolic outcome. Neutralization of CTLA4 and TGF-β partially abrogated the suppressive function of therapy-induced Tregs. Ablation or functional impairment of $Foxp3^+$ Tregs *in vivo* at start or stop of therapy impaired immune tolerance, highlighting the dependence of the therapy-induced tolerance in new-onset diabetic mice on the presence and functionality of $CD4^+Foxp3^+$ T cells. Biomarkers identified in this study can potentially be used in the future to tailor the *L. lactis*-based combination therapy for individual patients.

Clinical translation of antigen-based therapies has been disappointing so far, and specifically in autoimmune type 1 diabetes (T1D) the administration of oral insulin or glutamic acid decarboxylase (GAD) has not been efficacious in preventing or halting the disease in high-risk individuals or in new-onset patients to date (1-3). Issues like route and timing of vaccination, dosing strategy, but also reliability of delivery of full protein or peptide due to gastric digestion may lie at the basis of these failures (4). The introduction of a delivery vehicle like the gram-positive food-grade lactic acid bacterium *Lactococcus lactis* (*L. lactis*), able to deliver intact antigen and immunomodulating cytokines directly into the gut, in proximity to the gut-associated lymphoid tissue, is an appealing tool (5; 6). Another reason why antigen-based therapies did not succeed in stopping ongoing autoimmune processes may be that by the time the disease manifests the strong pathogenic immune reactions overpower the regulatory mechanisms induced by the therapy. In light of this consideration, we and others advocate that combinations of robust antigen-based interventions and systemic immune modulators may ultimately be needed to successfully reinstate long-term tolerance in ongoing autoimmunity without compromising immune function (7; 8). Previously, we reported that a combination therapy consisting of a 5-day course of anti-CD3 antibodies at disease onset along with a 6-week oral administration of live genetically modified *L. lactis* producing human pro-insulin (PINS) and IL10 safely restored durable normoglycemia in approximately 60% of non-obese diabetic (NOD) mice and elicited forkhead box p3 (Foxp3)-positive T cells with a regulatory phenotype (9). The route to bring this successful antigen-based therapy to new-onset T1D patients will depend both on the generation of a clinical-grade self-containing *L. lactis* strain (10) but also on a profound understanding of the processes underlying this disease-modifying approach and consequently on the implementation of certified biomarkers of both immune and therapeutic success.

Here, we demonstrated similar therapeutic efficacy in autoimmune diabetes remission using a clinical-grade self-containing *L. lactis* vaccine compared with the plasmid-driven *L. lactis* strain reported previously (9). In addition, we identified both functional beta cell reserve (initial blood glucose

concentrations <350 mg/dl) and pre-therapy insulin autoantibody (IAA) positivity as predictors of therapeutic efficacy and proved that $Foxp3^+$ T cells are prerequisite for the induction and maintenance of active tolerance induced by the *L. lactis*-based therapy.

Research Design and Methods

Mice.

NOD mice, originally obtained from Dr. Wu (Department of Endocrinology, Peking Union Medical College Hospital, Beijing, China), were housed and inbred in the animal facility of KU LEUVEN since 1989. NOD.Foxp3.DTR mice and NOD.Foxp3.hCD2 mice were bred from stocks kindly provided by Dr. Benoist (Harvard Medical School, Boston, MA) and Dr. Hori (RIKEN Research Center for Allergy and Immunology, Yokohama, Japan) respectively. Housing of all mice occurred under semi-barrier conditions, and animals were fed sterile food and water ad libitum. Mice were screened for the onset of diabetes by evaluating glucose levels in urine (Diastix® Reagent strips, Bayer, Leverkusen, Germany) and venous blood (AccuCheck®, Roche Diagnostics, Vilvoorde, Belgium). Mice were diagnosed as diabetic when having glucosuria and two consecutive blood glucose measurements exceeding 200 mg/dl. NOD-scid and NOD-scid γc -/- mice were bred from stocks purchased from the Jackson Laboratory (Bar Harbor, ME). Animals were maintained in accordance with the National Institutes of Health Guide for the Care and Use of Laboratory Animals, and all experimental procedures were approved and performed in accordance with the Ethics Committees of the KU Leuven (Leuven, Belgium) under project number 185-2009.

Bacteria and media.

Details on the construction, culture and *in vitro* quantification of the lactococcal vectors used in the present study are available in the Supplemental Research Design and Methods (9). For intragastric inoculations, stock suspensions were diluted 1000-fold in growth media and incubated for 16 hours at 30°C, reaching a saturation density of 2×10^9 cfu/ml. Bacteria were harvested by centrifugation and concentrated 10-fold in BM9 medium. Treatment doses consisted of 100 µl of this bacterial suspension.

New-onset diabetes intervention.

Upon diabetes determination, NOD or NOD transgenic mice were treated for 5 consecutive days intravenously (i.v.) (day 0-4; 2.5 µg/mouse) with hamster anti-mouse CD3 antibodies (clone 145-2C11, BioXCell, West Lebanon, NH). This therapy was given in combination with oral administration of either plasmid-driven or clinical-grade *L. lactis* strains (2×10^9 cfu) 5 times per week during 6 weeks. Control mice were left untreated. Individual blood glucose concentrations at the start of treatment were recorded. Mice were tested 3 times weekly for their weight and blood glucose status. Remission was defined as the absence of glucosuria and a return to normal blood glucose concentrations. Experimental animals were sacrificed immediately or long after stopping therapy (6 or 14 weeks after treatment initiation). Peripheral blood, lymph organs and pancreas were harvested, and single cells were assessed for phenotyping as described in the Supplemental Research Design and Methods. Detailed methodology and references on *in vitro* suppression assays are described in the Supplemental Research Design and Methods. Mice were removed from the study prior to the 14-week endpoint when blood glucose concentrations exceeded 600 mg/dl in two consecutive measurements.

Glucose tolerance test.

One or two weeks prior to sacrifice intraperitoneal glucose tolerance tests (IPGTT) were performed. Mice were fasted for 16 hours, injected intraperitoneally (i.p.) with glucose (2 g/kg) and blood glucose concentrations were measured at 0, 15, 30, 60, 90 and 120 minutes.

IAA measurement.

Heparinized plasma was collected from new-onset diabetic NOD mice before treatment randomization and at therapy discontinuation, and IAAs were analyzed at the UF Department of Pathology, Immunology and Laboratory Medicine, College of Medicine, Gainesville, Florida, as described (11).

In vivo blocking of CTLA4 and TGF-β.

Mice tolerized by *L. lactis*-based therapy were injected intraperitoneally (i.p.) after therapy withdrawal with blocking antibodies against CTLA4 (clone UC10-4F10, Bioceros) and TGF-β (clone 1D11.16.8, BioXCell) in the following dose regimen: 250 µg at day 1 and 3 and then 100 µg at day 6, 8, 10, 13 and 18 for CTLA4; 200 µg 3 times per week during 3 weeks for TGF-β. Blood glucose concentrations were measured daily up to 25 days after first injection.

Adoptive transfer of diabetes.

To assess the diabetogenic potential of Teff cells, total T cells from spleen (1×10^7 cells) of new-onset diabetic controls, responders and non-responders of *L. lactis*-based therapy were transferred i.v. into the tail veins of 6- to 8-week-old immune-deficient NOD-scid mice. Recipient mice were monitored twice weekly for the development of diabetes up to 100 days post-cell transfer.

DT-mediated depletion of Foxp3$^+$ T cells in NOD.Foxp3.DTR mice.

NOD.Foxp3.DTR mice (expressing the human diphtheria toxin receptor (DTR) under the control of Foxp3 transcriptional control elements) allow for the depletion of Foxp3$^+$ T cells upon DT administration (12). For Treg depletion, NOD.Foxp3.DTR mice (unmanipulated or tolerized after stopping the *L. lactis-based therapy*) were injected i.p. with 40 µg/kg bodyweight of DT (Sigma) on days 1, 2, 4, and 7 and examined on day 8. Following DT injections, weight, urine and blood glucose status of mice were monitored. Foxp3$^+$ T cells were monitored in peripheral blood and pancreas by flow cytometry and histology respectively as described (13).

FOXP3-inhibitory peptide P60 in combination with L. lactis-based therapy

P60 (a 15-mer synthetic peptide that can bind to and block FOXP3, i.p. 50 µg/dose daily, up to 14 doses) was given at start of the *L. lactis*-based therapy, as previously described (14).

Histology of pancreas and insulitis grading.

Six-µm sections from formalin-fixed paraffin-embedded pancreas tissues were cut and collected 100-µm apart, then stained with hematoxylin eosin. Islets were observed under light microscopy at 20× or 40×, enumerated and graded by an independent investigator in blinded fashion. At least 25 islets per pancreatic sample were scored for islet infiltration as follows: 0, no infiltration; 1, peri-insulitis; 2, islets with lymphocyte infiltration in less than 50% of the area, 3, islets with lymphocyte infiltration in more than 50% of the area or completely destroyed.

Islet-resident Foxp3$^+$ T cell detection.

Pancreas tissues were snap-frozen in 2-methyl-butane 99% (ACROS Organics, Geel, Belgium), and cut into 12-µm tissue sections. Foxp3$^+$ T cell detection was performed as described (9).

Statistics.

All data were analyzed using GraphPad Prism 6 (Graphpad Prism, La Jolla, CA). Survival curves were computed with Kaplan-Meier test and compared with log-rank test. Groups were analyzed by ANOVA (non-parametric Kruskal-Wallis test) with Dunn's multiple comparison or with Mann-Whitney U test, as appropriate. Error bars represent SEM. Unless otherwise indicated, differences are not significant (ns). * P <0.05, ** P <0.01, *** P <0.001, **** P < 0.0001.

Results

A clinical-grade self-containing L. lactis vaccine combined with low-dose anti-CD3 stably reverts new-onset diabetes, preserves residual beta cell function and halts insulitis progression in NOD mice.

Using a clinical-grade self-containing *L. lactis* strain secreting human PINS along with IL10 in combination with sub-therapeutic doses of anti-CD3 antibodies, 66% (23 out of 35) of mice reverted to normoglycemia for at least 14 weeks after disease onset, which was significantly superior to 43% of mice treated by anti-CD3 alone (**Fig. 1A**). This therapeutic efficacy obtained with the clinical-grade *L. lactis* strain was comparable to the combination therapy with plasmid-driven *L. lactis* strain (72%, 18 out of 25 mice, ns). As expected, animals left untreated (n=20) or treated with the empty vector bacterial strain *L. lactis*-pT1NX (n=9) remained hyperglycemic and were sacrificed when 20% of their starting body weight was lost. Monotherapy with either the clinical-grade or plasmid-driven *L. lactis* strain secreting PINS and IL10 was significantly less effective than the combination with anti-CD3 (0% (n=8) and 17% (n=8) respectively)(**Fig. 1A**).

During follow up, new-onset diabetic controls and mice protected or not by *L. lactis*-based therapy were subjected to IPGTT and sacrificed 6 weeks after treatment initiation at which time their pancreas tissues were assessed by histology. Only in the successfully treated animals, residual beta cell function (i.e. assessed as area under glucose tolerance curve (AUCglucose)) was preserved and smaller proportions of islets had severe insulitis (**Fig. 1B**). Of interest, at the end of the combination therapy no difference in the severity of insulitis was observed between responders and non-responders (**Fig. 1C)**.

Starting glycemia and IAA positivity predict therapeutic success of L. lactis-based therapy.

No influence of age or gender of mice was observed on therapeutic success of the *L. lactis*-based therapy (data not shown). However, as shown previously (9), glycemic concentrations at the beginning

of therapy predicted success, with 82% of mice starting with a glycemia below 350 mg/dl cured (n=22), in comparison to 38% of mice with a starting glycemia above 350 mg/dl (n=13) (**Fig. 2A**). In addition, positivity for IAAs at entry seemed to correlate with therapeutic success (**Fig. 2B**). Interestingly, mice with blood glucose concentrations <350 mg/dl and IAA positivity at therapy start had a clearly superior diabetes remission rate (89%, n = 8) than mice with blood glucose levels >350 mg/dl and being IAA negative (33%; n = 5; P=0.07)(**Fig. 2C**). Moreover, the *L. lactis*-based therapy significantly decreased IAA levels, particularly in mice responsive to the therapy (**Fig. 2D**).

L. lactis-based therapy induces higher levels of Foxp3$^+$ T cells with regulatory capacity but no changes in Teff cells.

The mechanisms underlying disease remission induced by the *L. lactis*-based treatment were investigated by dissociating between the therapeutic immune effects in mice responsive or not to the intervention. We found that the percentages of CD4$^+$Foxp3$^+$ (both CD25$^+$ and CD25$^-$) T cells observed in the peripheral blood (**Fig. 3A**), the pancreatic draining lymph nodes (**Fig. 3B**), and the pancreas (**Fig. 3C**) were significantly higher in mice treated with the *L. lactis*-based therapy in comparison to untreated controls. Interestingly, in the pancreatic draining lymph nodes and pancreas, but not in peripheral blood, the increased frequency of CD4$^+$Foxp3$^+$ T cells was less pronounced in responders than non-responders. Using multicolor flow cytometry, we identified that most CD4$^+$Foxp3$^+$ Tregs were positive for CTLA4 and that the expression of this inhibitory marker was significantly higher in pancreatic draining lymph nodes (for both responders and non-responders) and pancreas (only for responders) of treated mice compared to untreated controls (**Supplemental Fig. S1B** and **1C**). Of interest, no differences in the percentages of CD4$^+$Foxp3$^+$CTLA4$^+$ T cells were observed in the peripheral blood of treated mice compared to untreated controls (**Fig. 3D**).

The percentages of naïve ($CD44^-CD62L^+CCR7^+$), effector memory ($CD44^+CD62L^-CCR7^-$) and central memory ($CD44^+CD62L^+CCR7^+$) $CD4^+$ T cells were not altered in any recipient group with respect to therapeutic success or failure (data not shown). Transfer of splenocytes from responders and non-responders of *L. lactis*-based treatment caused diabetes in NOD-scid recipients with similar disease kinetics as transfer of splenocytes isolated from untreated new-onset diabetic controls, suggesting that circulating diabetogenic cells were not depleted from treated mice (**Supplemental Fig. S2**).

Diabetes reversal induced by L. lactis-based therapy is accompanied by and depends on the generation of functional $Foxp3^+$ Tregs.

Using NOD.Foxp3.hCD2 mice treated by *L. lactis*-based therapy, we could isolate $CD4^+CD25^+Foxp3^+$ T cells for functional *in vitro* studies, in which they suppressed proliferation, CD69 activation and IFN-γ production of pathogenic $CD4^+CD25^-$ Teff cells. These Tregs produced IL10 (and TGF-β) when they were co-cultured and stimulated with anti-CD3 antibody in the presence of splenic antigen-presenting cells (APCs) isolated from NOD-scid γc -/- mice (**Fig. 4** and data not shown). No difference in regulatory capacity of $CD4^+CD25^-Foxp3^+$ T cells was seen between therapy responders and non-responders.

Addition of anti-CTLA4 Ig (clone UC10-4F10) or a TGF-β neutralizing antibody (clone 1D11.16.8) significantly reduced the suppression by the $CD4^+CD25^+Foxp3^+$ T cells (**Fig. 5A**), suggesting that $CD4^+CD25^+Foxp3^+$ Tregs of cured mice inhibit Teff proliferation via a CTLA4- and TGF-β-dependent fashion *in vitro*. Adding anti-IL10 (clone JES5-2A5) did not alter the direct suppressive effect of the Tregs. On the other hand, these regulatory mechanisms were not demonstrated with the $CD4^+CD25^-Foxp3^+$ T cell fraction from therapy responders and non-responders (**Fig. 5B**). Treating stably cured

mice *in vivo* with a combination of anti-CTLA4 Ig (clone UC10-4F10) and anti-TGF-β (clone 1D11.16.8) led to diabetes recurrence in 2 out of 5 mice (**Fig. 5C**).

Finally, we investigated whether the therapeutic success of *L. lactis*-based therapy was depended on the presence and functionality of $Foxp3^+$ T cells. For this, new-onset diabetic NOD mice were simultaneously treated with the *L. lactis*-based therapy and the FOXP3-inhibitory peptide P60 for a period of 14 days (**Fig. 6A**). Interestingly, none of the mice (n=6) developed normoglycemia, while mice treated with the *L. lactis*-based therapy and vehicle (n=11) had already a 60% diabetes remission rate, indicating that Tregs are crucial for induction of therapy-induced tolerance (**Fig. 6B**).

Next, new-onset (spontaneously) diabetic NOD.Foxp3.DTR mice were treated with the *L. lactis*-based therapy and after stable diabetes reversal was observed, $Foxp3^+$ T cells were eliminated using DT as described in the scheme depicted in **Fig. 7A**. First, we established in unmanipulated NOD.Foxp3.DTR mice that the selected DT regimen eliminated over 90% of $CD4^+Foxp3^+$ T cells, with the remaining Tregs expressing low or no CD25, in the peripheral blood within 3 days after first DT injection (**Supplemental Fig. S3A-C**). A progressive repopulation of these cells started from day 5 after first DT injection as has been reported for several Foxp3.DTR strains (15-17). This DT regimen also dramatically decreased the amount of $Foxp3^+$ T cells residing in the pancreas, consequently leading to the development of autoimmune diabetes (**Supplemental Fig. S3B and S2D**). Next, comparable to wild-type NOD mice, the *L. lactis*-based treatment induced autoimmune diabetes remission in 57% of NOD.Foxp3.DTR mice (4 out of 7 mice)(**Fig. 7B**). Transient $Foxp3^+$ T cell depletion resulted in a complete reversal to the diabetic state in all mice (n=4) that were initially cured by the therapy, as evidenced by the reappearance of glucosuria along with severe hyperglycemia starting from day 2 after first DT injection (**Fig. 7B**). This breach of immune tolerance to insulin-producing beta cells was also accompanied by the induction of severe insulitis (**Fig. 7C**) and the ablation of the islet-resident $Foxp3^+$ Treg pool (**Fig. 7D**). Collectively, these data demonstrated that the therapeutic effect from the *L. lactis*-based intervention depended on the presence and functionality of $Foxp3^+$ Tregs.

Discussion

Oral tolerance as a means of intervention to arrest disease has been extensively explored in various animal models of autoimmune disease including T1D (18). We previously described reversal of new-onset autoimmune diabetes in mice by the oral administration of plasmid-driven *L. lactis* strains secreting diabetes-relevant antigens (i.e. whole PINS or GAD65 peptide) and IL10 in combination with systemic low-dose anti-CD3 (9; 11). In both antigen-based therapies, induction of $CD4^+CD25^+Foxp3^+$ T cells accompanied the therapeutic success.

In the current study, we designed an oral clinical-grade self-containing *L. lactis* strain secreting chromosomal-integrated human PINS and IL10. When combined with a short course of sub-therapeutic doses of anti-CD3, the intervention was safe and highly effective in inducing long-term normoglycemia in new-onset diabetic mice. Initial blood glucose concentrations (<350 mg/dl) in addition to IAA positivity at disease onset were predictors of therapeutic outcome, while preservation of residual beta cell function and decline in IAA positivity were markers of therapeutic success. It is encouraging that studies with anti-CD3 monotherapy in new-onset T1D patients already revealed that subjects enrolled within 6 weeks of diagnosis and with higher levels of C-peptide at entry responded better to therapy (19-21). These observations suggest that some degree of residual beta cell mass will be necessary for therapeutic success when intervening at the moment of diabetes diagnosis, namely when dysglycemia is present. Likewise, a post-hoc analysis of new-onset T1D participants of the otelixizumab trial found a good correlation between pre-existing IAA levels and clinical outcome (22). IAA positivity at study entry was also found to distinguish responders from non-responders among recipients of oral insulin (1).

Our previous studies suggested that the mechanism of *L. lactis*-based therapy involved the induction of $CD4^+CD25^+Foxp3^+$ T cells (9). By dissociating between the immune effects of the *L. lactis*-based

intervention in mice responsive or not to the therapy, we were able to further characterize the nature and role of the immune processes accompanying the treatment. The *L. lactis*-based therapy induced suppressive IL10-secreting $CD4^+Foxp3^+$ (both $CD25^+$ and $CD25^-$) T cells in the pancreatic draining lymph nodes and pancreas of responders and even more so of non-responders, suggesting enhanced recruitment of Tregs to the inflamed target tissues. In the periphery, the frequency of $CD4^+Foxp3^+$ T cells was also increased in treated mice compared to untreated controls, pointing towards possible value for this cell population as immune marker. Interestingly, the frequency of $CTLA4^+$ T cells among various Treg subsets was significantly higher in the pancreas of combination therapy-treated responder mice compared to new-onset diabetic mice and in contrast to combination therapy-treated non-responder mice. CTLA4 by Tregs has a non-redundant role to limit lymphopenia-induced uncontrolled proliferation of autoreactive Teff cells *in vivo* (23). Alternatively, CTLA4 by Tregs may prolong the contact time between Tregs and dendritic cells via LFA1 activation (24), increasing the efficiency of Treg suppression in a (transient) lymphopenic environment as the one induced by low-dose anti-CD3. As various immune or tissue-specific mediators are important for Treg suppressive function at these inflammatory sites, more in-depth studies looking at expression of chemokines, adhesion molecules and extracellular matrix components of site-specific effector Tregs can provide more insights in follow-up studies. Of note, no difference was seen in the degree of insulitis between responder and non-responder mice, suggesting also alterations in other lymphocyte subsets besides Tregs.

It is still not fully understood how Tregs control immune effector responses in autoimmune diseases and inflammation. Several studies demonstrated that peripheral Tregs can use different regulatory mechanisms according to their environmental milieu and stimulatory conditions (25). In our case, CTLA4 and TGF-β were important for the regulatory activity of therapy-expanded $CD4^+CD25^+Foxp3^+$ T cells *in vitro* and partially *in vivo*, while IL10 was not. There is no consensus on the role of CTLA4 for Treg function and several effects have been reported; induction of cell-intrinsic negative signals to activated Teff cells, modulation of APCs' development and stable function

of Foxp3$^+$ Tregs (26; 27). With regard to the involvement of TGF-β in therapy-mediated suppression, this cytokine can regulate several immunological processes, such as inflammation, lineage commitment, antibody generation as well as tolerance induction (28). Moreover, it can preserve Foxp3 expression and support the differentiation of other T cells into Treg-like cells (29). In fact, TGF-β can promote the development of IL10-secreting Tregs, as treatment of mice with anti-TGF-β prevented the conversion of CD4$^+$Foxp3$^-$ cells into CD4$^+$Foxp3$^+$IL10$^+$ cells in intestine-associated lymphoid tissues (30). Although IL10 seemed to be a good marker for the identification of our *L. lactis*-based therapy-induced Tregs, the role of IL10 in their regulator function remains controversial. Others also demonstrated that anti-IL10 antibodies did not abrogate established tolerance *in vivo* (31). Here, it has been discussed whether IL10 modulated the APCs' maturation phenotype inducing anergy in both antigen-specific CD4$^+$ and CD8$^+$ T cells and preferentially converting truly naïve CD4$^+$ T cells into suppressor cells expressing Foxp3, rather than through direct activity on T cells (32). Based on our observations, it is intriguing to speculate that Treg production of IL10 is a major mechanism by which Tregs regulate inflammation at environmental interfaces, whereas TGF-β and CTLA4-dependent regulation of APCs' function may be a regulatory mechanism that predominates in secondary lymphoid tissues where it controls the initial activation and expansion of naïve autoreactive T-cells.

As in mice, human Tregs are defined by having a suppressive phenotype endowed by high and sustained expression of the transcription factor Foxp3 (33) and loss of function/mutation in the Foxp3 gene leads to severe fatal autoimmune disorders (15; 34). In the current study, we discovered that the specific inhibition of Treg functionality by the P60 peptide (14) at the start of *L. lactis*-based therapy completely impaired the induction of therapy-induced tolerance. Moreover, transient depletion of Foxp3$^+$ Tregs from therapy-tolerized NOD.Foxp3.DTR mice was sufficient to induce complete disease relapse in all animals, demonstrating that the presence of Foxp3$^+$ T cells was crucial to maintain therapeutic tolerance and control pathogenic Teff cells which were still present in mice responsive to *L. lactis*-based therapy. A recent study suggested that antigen-specific Foxp3$^+$ Tregs can also mediate

tolerance both by diminishing recruitment of antigen-carrying inflammatory APCs to lymph nodes and by impairing their function (35).

In conclusion, our data demonstrated that combining a clinical-grade self-containing *L. lactis* secreting human PINS and IL10 with low-dose anti-CD3 increased the frequency of diabetes reversal compared to anti-CD3 mono-therapy. Both therapy responders and non-responders had increased frequencies of $CD4^+Foxp3^+$ T cells, suggesting that immune effects induced by the *L. lactis*-based therapy occurred in each individual recipient, but that therapeutic success (defined as return to stable normoglycemia) depended on other parameters, such as functional beta cell mass still present at disease onset. This idea was further strengthened by the observation that therapeutic success was correlated with starting glycemia. Next to initial blood glucose concentrations at entry, also IAA levels predicted outcome of this *L. lactis*-based therapy using PINS as antigen. Finally, we showed that $Foxp3^+$ Tregs were essential to induce and maintain active tolerance and control diabetogenic immune responses in tolerized mice. These findings provide all the ingredients for testing this intervention in humans: a clinical-grade self-containing *L. lactis* secreting islet antigen(s), biomarkers for predicting therapeutic success, and the demonstration that the induction of $Foxp3^+$ T cells is the basis of the *L. lactis*-based therapy-induced cure.

Authors' contributions

T.T: design, experiments, interpretation of data, drafting of the manuscript; D.P.C: design, experiments, interpretation of data, critical revision of article; H.K: critical revision of article; G.S: experiments; F.M.: experiments; J.P.M.C.M.C: experiments; L.S: critical revision of article; P.R: critical revision of article; C.W: experiments, critical revision of article; N.C: critical revision of article; J.J.L: critical revision of article; F.D: critical revision of article, interpretation of data; C.G: idea, design, interpretation of data, drafting of the manuscript; C.M: idea, design, interpretation of data, drafting of the manuscript. C.M and C.G stand as guarantors for the study.

Acknowledgements

We thank Sofie Robert, Jos Laureys and Elien De Smidt (CEE, KU Leuven, Belgium) for excellent technical support. This work was supported by grants from the European Community's Health Seventh Framework Programme (FP7/2009-2014 under grant agreement 241447 with acronym NAIMIT), the Juvenile Diabetes Research Foundation (JDRF 17-2011-524), the Fund for Scientific Research Flanders (FWO-Vlaanderen G.0554.13N), the KU Leuven (GOA 2014/010), and the EFSD/Sanofi Innovative Approaches Programme 2014 and by gifts for Hippo & Friends Type 1 Diabetes Fonds and Carpe Diem Fonds voor Diabetesonderzoek. D.P.C is a PhD fellow of the FWO-Vlaanderen (11Y6716N). H.K is a postdoctoral fellow and C.M a clinical researcher of the FWO-Vlaanderen. F.D received support from the Italian Ministry of Research (n. 2010JS3PMZ_008), the Italian Ministry of Health, and from Fondazione Roma.

Disclosure

L.S and P.R have financial interests in Intrexon Actobiotics NS, including employment and stock options. Otherwise we declare no conflict of interest.

References

1. Skyler JS, Krischer JP, Wolfsdorf J, Cowie C, Palmer JP, Greenbaum C, Cuthbertson D, Rafkin-Mervis LE, Chase HP, Leschek E: Effects of oral insulin in relatives of patients with type 1 diabetes: The Diabetes Prevention Trial--Type 1. Diabetes care 2005;28:1068-1076

2. Wherrett DK, Bundy B, Becker DJ, DiMeglio LA, Gitelman SE, Goland R, Gottlieb PA, Greenbaum CJ, Herold KC, Marks JB, Monzavi R, Moran A, Orban T, Palmer JP, Raskin P, Rodriguez H, Schatz D, Wilson DM, Krischer JP, Skyler JS, Type 1 Diabetes TrialNet GADSG: Antigen-based therapy with glutamic acid decarboxylase (GAD) vaccine in patients with recent-onset type 1 diabetes: a randomised double-blind trial. Lancet 2011;378:319-327

3. Ludvigsson J, Krisky D, Casas R, Battelino T, Castano L, Greening J, Kordonouri O, Otonkoski T, Pozzilli P, Robert JJ, Veeze HJ, Palmer J, Samuelsson U, Elding Larsson H, Aman J, Kardell G, Neiderud Helsingborg J, Lundstrom G, Albinsson E, Carlsson A, Nordvall M, Fors H, Arvidsson CG, Edvardson S, Hanas R, Larsson K, Rathsman B, Forsgren H, Desaix H, Forsander G, Nilsson NO, Akesson CG, Keskinen P, Veijola R, Talvitie T, Raile K, Kapellen T, Burger W, Neu A, Engelsberger I, Heidtmann B, Bechtold S, Leslie D, Chiarelli F, Cicognani A, Chiumello G, Cerutti F, Zuccotti GV, Gomez Gila A, Rica I, Barrio R, Clemente M, Lopez Garcia MJ, Rodriguez M, Gonzalez I, Lopez JP, Oyarzabal M, Reeser HM, Nuboer R, Stouthart P, Bratina N, Bratanic N, de Kerdanet M, Weill J, Ser N, Barat P, Bertrand AM, Carel JC, Reynaud R, Coutant R, Baron S: GAD65 antigen therapy in recently diagnosed type 1 diabetes mellitus. N Engl J Med 2012;366:433-442

4. Culina S, Boitard C, Mallone R: Antigen-based immune therapeutics for type 1 diabetes: magic bullets or ordinary blanks? Clin Dev Immunol 2011;2011:286248

5. Steidler L, Rottiers P: Therapeutic drug delivery by genetically modified Lactococcus lactis. Annals of the New York Academy of Sciences 2006;1072:176-186

6. Robert S, Steidler L: Recombinant Lactococcus lactis can make the difference in antigen-specific immune tolerance induction, the Type 1 Diabetes case. Microb Cell Fact 2014;13 Suppl 1:S11

7. Matthews JB, Staeva TP, Bernstein PL, Peakman M, von Herrath M, Group I-JTDCTA: Developing combination immunotherapies for type 1 diabetes: recommendations from the ITN-JDRF Type 1 Diabetes Combination Therapy Assessment Group. Clinical and experimental immunology 2010;160:176-184

8. Robert S, Korf H, Gysemans C, Mathieu C: Antigen-based vs. systemic immunomodulation in type 1 diabetes: the pros and cons. Islets 2013;5:53-66

9. Takiishi T, Korf H, Van Belle TL, Robert S, Grieco FA, Caluwaerts S, Galleri L, Spagnuolo I, Steidler L, Van Huynegem K, Demetter P, Wasserfall C, Atkinson MA, Dotta F, Rottiers P, Gysemans C, Mathieu C: Reversal of autoimmune diabetes by restoration of antigen-specific tolerance using genetically modified Lactococcus lactis in mice. J Clin Invest 2012;122:1717-1725

10. Steidler L, Neirynck S, Huyghebaert N, Snoeck V, Vermeire A, Goddeeris B, Cox E, Remon JP, Remaut E: Biological containment of genetically modified Lactococcus lactis for intestinal delivery of human interleukin 10. Nat Biotechnol 2003;21:785-789

11. Robert S, Gysemans C, Takiishi T, Korf H, Spagnuolo I, Sebastiani G, Van Huynegem K, Steidler L, Caluwaerts S, Demetter P, Wasserfall CH, Atkinson MA, Dotta F, Rottiers P, Van Belle TL,

Mathieu C: Oral Delivery of Glutamic Acid Decarboxylase (GAD)-65 and IL10 by Lactococcus lactis Reverses Diabetes in Recent-Onset NOD Mice. Diabetes 2014;63:2876-2887

12. Feuerer M, Shen Y, Littman DR, Benoist C, Mathis D: How punctual ablation of regulatory T cells unleashes an autoimmune lesion within the pancreatic islets. Immunity 2009;31:654-664

13. Tian L, Altin JA, Makaroff LE, Franckaert D, Cook MC, Goodnow CC, Dooley J, Liston A: Foxp3(+) regulatory T cells exert asymmetric control over murine helper responses by inducing Th2 cell apoptosis. Blood 2011;118:1845-1853

14. Casares N, Rudilla F, Arribillaga L, Llopiz D, Riezu-Boj JI, Lozano T, Lopez-Sagaseta J, Guembe L, Sarobe P, Prieto J, Borras-Cuesta F, Lasarte JJ: A peptide inhibitor of FOXP3 impairs regulatory T cell activity and improves vaccine efficacy in mice. Journal of immunology 2010;185:5150-5159

15. Kim JM, Rasmussen JP, Rudensky AY: Regulatory T cells prevent catastrophic autoimmunity throughout the lifespan of mice. Nature immunology 2007;8:191-197

16. Suffner J, Hochweller K, Kuhnle MC, Li X, Kroczek RA, Garbi N, Hammerling GJ: Dendritic cells support homeostatic expansion of Foxp3+ regulatory T cells in Foxp3.LuciDTR mice. Journal of immunology 2010;184:1810-1820

17. Mayer CT, Lahl K, Milanez-Almeida P, Watts D, Dittmer U, Fyhrquist N, Huehn J, Kopf M, Kretschmer K, Rouse B, Sparwasser T: Advantages of Foxp3(+) regulatory T cell depletion using DEREG mice. Immun Inflamm Dis 2014;2:162-165

18. Commins SP: Mechanisms of Oral Tolerance. Pediatr Clin North Am 2015;62:1523-1529

19. Sherry N, Hagopian W, Ludvigsson J, Jain SM, Wahlen J, Ferry RJ, Jr., Bode B, Aronoff S, Holland C, Carlin D, King KL, Wilder RL, Pillemer S, Bonvini E, Johnson S, Stein KE, Koenig S, Herold KC, Daifotis AG, Protege Trial I: Teplizumab for treatment of type 1 diabetes (Protege study): 1-year results from a randomised, placebo-controlled trial. Lancet 2011;378:487-497

20. Keymeulen B, Vandemeulebroucke E, Ziegler AG, Mathieu C, Kaufman L, Hale G, Gorus F, Goldman M, Walter M, Candon S, Schandene L, Crenier L, De Block C, Seigneurin JM, De Pauw P, Pierard D, Weets I, Rebello P, Bird P, Berrie E, Frewin M, Waldmann H, Bach JF, Pipeleers D, Chatenoud L: Insulin needs after CD3-antibody therapy in new-onset type 1 diabetes. N Engl J Med 2005;352:2598-2608

21. Herold KC, Gitelman SE, Willi SM, Gottlieb PA, Waldron-Lynch F, Devine L, Sherr J, Rosenthal SM, Adi S, Jalaludin MY, Michels AW, Dziura J, Bluestone JA: Teplizumab treatment may improve C-peptide responses in participants with type 1 diabetes after the new-onset period: a randomised controlled trial. Diabetologia 2013;56:391-400

22. Demeester S, Keymeulen B, Kaufman L, Van Dalem A, Balti EV, Van de Velde U, Goubert P, Verhaeghen K, Davidson HW, Wenzlau JM, Weets I, Pipeleers DG, Gorus FK: Preexisting insulin autoantibodies predict efficacy of otelixizumab in preserving residual beta-cell function in recent-onset type 1 diabetes. Diabetes care 2015;38:644-651

23. Sojka DK, Hughson A, Fowell DJ: CTLA-4 is required by CD4+CD25+ Treg to control CD4+ T-cell lymphopenia-induced proliferation. European journal of immunology 2009;39:1544-1551

24. Balkow S, Heinz S, Schmidbauer P, Kolanus W, Holzmann B, Grabbe S, Laschinger M: LFA-1 activity state on dendritic cells regulates contact duration with T cells and promotes T-cell priming. Blood 2010;116:1885-1894

25. Liston A, Gray DH: Homeostatic control of regulatory T cell diversity. Nature reviews Immunology 2014;14:154-165

26. Tang Q, Boden EK, Henriksen KJ, Bour-Jordan H, Bi M, Bluestone JA: Distinct roles of CTLA-4 and TGF-beta in CD4+CD25+ regulatory T cell function. European journal of immunology 2004;34:2996-3005

27. Wing K, Yamaguchi T, Sakaguchi S: Cell-autonomous and -non-autonomous roles of CTLA-4 in immune regulation. Trends in immunology 2011;32:428-433

28. Tran DQ: TGF-beta: the sword, the wand, and the shield of FOXP3(+) regulatory T cells. Journal of molecular cell biology 2012;4:29-37

29. Selvaraj RK, Geiger TL: A kinetic and dynamic analysis of Foxp3 induced in T cells by TGF-beta. Journal of immunology 2007;178:7667-7677

30. Maynard CL, Harrington LE, Janowski KM, Oliver JR, Zindl CL, Rudensky AY, Weaver CT: Regulatory T cells expressing interleukin 10 develop from Foxp3+ and Foxp3- precursor cells in the absence of interleukin 10. Nature immunology 2007;8:931-941

31. Fowler S, Powrie F: CTLA-4 expression on antigen-specific cells but not IL-10 secretion is required for oral tolerance. European journal of immunology 2002;32:2997-3006

32. Pletinckx K, Dohler A, Pavlovic V, Lutz MB: Role of dendritic cell maturity/costimulation for generation, homeostasis, and suppressive activity of regulatory T cells. Front Immunol 2011;2:39

33. Hori S, Nomura T, Sakaguchi S: Control of regulatory T cell development by the transcription factor Foxp3. Science 2003;299:1057-1061

34. Mayer CT, Ghorbani P, Kuhl AA, Stuve P, Hegemann M, Berod L, Gershwin ME, Sparwasser T: Few Foxp3(+) regulatory T cells are sufficient to protect adult mice from lethal autoimmunity. European journal of immunology 2014;44:2990-3002

35. Alissafi T, Hatzioannou A, Ioannou M, Sparwasser T, Grun JR, Grutzkau A, Verginis P: De novo-induced self-antigen-specific Foxp3+ regulatory T cells impair the accumulation of inflammatory dendritic cells in draining lymph nodes. Journal of immunology 2015;194:5812-5824

Figure legends

Figure 1 – A clinical-grade self-containing *L. lactis* vaccine combined with low-dose anti-CD3 stably reverts new-onset diabetes, preserves residual beta cell function and halts insulitis progression in NOD mice. New-onset diabetic NOD mice were treated as indicated and blood glucose concentrations were followed up for 14 weeks post-treatment initiation (**A**) Shown is the percentage of mice that remained diabetic after treatment. †, dead or moribund mice. In all Kaplan-Meier survival curves, statistical significance between groups was determined by Mantel-Cox log-rank test; * $P < 0.05$, ****, $P < 0.0001$. (**B**) IPGTTs were performed on new-onset diabetic NOD mice in addition to *L. lactis*-based combination therapy (CT)-treated mice (both responders and non-responders) 1 to 2 weeks prior to treatment termination. Corresponding area under the glucose tolerance curve (AUCglucose; mg/dl × 120 minutes) over 2 hours is shown. (**C**) Insulitis scoring was performed in a blinded manner on paraffin-embedded pancreatic sections of new-onset diabetic and *L. lactis*-based combination therapy (CT)-treated mice (both responders and non-responders), as indicated, at the end of treatment. Statistical significance between groups was calculated using Mann-Whitney t-test; ** $P < 0.01$.

Figure 2 – Starting glycemia and IAA positivity at study entry predict therapeutic success of *L. lactis*-based combination therapy. (**A**) New-onset diabetic NOD mice were stratified based on starting blood glucose concentrations (b.g.) under or above 350 mg/dl at study entry. Shown is the percentage of mice that remained diabetic after combination treatment (CT) with the clinical-grade *L. lactis* strain. In the Kaplan-Meier survival curve, statistical significance between groups was determined by Mantel-Cox log-rank test; ** $P < 0.01$. (**B**) Before treatment randomization, the serum of each individual NOD mouse was collected to measure IAA levels in a blinded fashion. Percentage of mice responsive or not to *L. lactis*-based combination therapy for IAA positivity. (**C**) New-onset diabetic NOD mice were stratified based on starting blood glucose concentrations (b.g.) under or above

350 mg/dl and IAA status (positive or negative) at study entry. Shown is the percentage of mice that were tolerized after therapy. (**D**) IAA levels at diabetes diagnosis and after *L. lactis*-based combination treatment follow-up in therapy responders (upper panel) and non-responders (lower panel). Statistical significance between groups was calculated using Mann-Whitney t-test; ** $P < 0.01$. Starting glycemia and positivity for IAAs at entry correlated with therapeutic success. Change in IAA positivity between pre- and post-therapy was significantly different in therapy responders.

Figure 3 – *L. lactis*-based combination therapy induces higher levels of Foxp3$^+$ T cells in responders than in non-responders. The percentages of CD25$^+$Foxp3$^+$ cells (left panel), CD25$^-$ Foxp3$^+$ cells (middle panel), and total Foxp3$^+$ cells (right panel) within the CD4$^+$ T cell population in peripheral blood (**A**), pancreatic draining lymph nodes (**B**) and pancreas (**C**) of new-onset diabetic and *L. lactis*-based combination therapy (CT)-treated mice (both responders and non-responders). The percentages of CD25$^+$Foxp3$^+$CTLA4$^+$ cells (left panel), CD25$^-$Foxp3+CTLA4$^+$ cells (middle panel), and Foxp3$^+$CTLA4$^+$ cells (right panel) within the CD4$^+$ T cell population in peripheral blood (**D**), pancreatic draining lymph nodes (**E**) and pancreas (**F**) of new-onset diabetic and *L. lactis*-based combination therapy (CT)-treated mice (both responders and non-responders). Each symbol represents one mouse, and horizontal bars indicate the median value. Statistical significance was calculated using Mann-Whitney t-test; * $P < 0.05$, ** $P < 0.01$, ***, $P < 0.001$; ****, $P < 0.0001$.

Figure 4 – *L. lactis*-based combination therapy induces suppressive IL10-secreting Foxp3$^+$ T cells in responders and non-responders. *In vitro* polyclonal suppressor assay. CD4$^+$CD25$^-$ effector T cells (Teff) were isolated from normoglycemic NOD mice, dye-labeled, and stimulated for 72 hours using soluble anti-CD3 in the presence of accessory cells and increasing ratios of CD4$^+$CD25$^+$Foxp3$^+$ or CD4$^+$CD25$^-$Foxp3$^+$ T cells (Treg), isolated from *L. lactis*-based combination therapy (CT)-treated

NOD.Foxp3.hCD2 mice (both responders and non-responders) at the end of the indicated 6-week treatment. Proliferation of Teff cells was measured by flow cytometric analysis of dye dilution and shown as the percentage of Teff cells undergone 2 or more divisions, normalized to effector only culture. Activation of Teff cells was measured by flow cytometric analysis of CD69 and shown as the MFI, normalized to effector only culture. MSD high-sensitivity multiplex assay of IFN-γ and IL10 concentrations in the Treg:Teff cultures. Statistical significance between groups was calculated using Kruskal-Wallis test followed by Dunnett´s multiple testing; * $P < 0.05$, ** $P < 0.01$, ***, $P < 0.001$; * $P < 0.05$, ** $P < 0.01$.

Figure 5 – *L. lactis*-based combination therapy-induced Tregs depend on CTLA4 and TGF-β to control T effector cell responses. T effector (Teff) proliferation – shown as the percentage of Teff cells that had undergone 2 or more divisions, normalized to proliferation by effector only culture. Dye-labeled $CD4^+CD25^-$ T cells (Teff) were stimulated with anti-CD3 (0.5 µg/ml) in the presence of accessory cells and (**A**) $CD4^+CD25^+Foxp3^+$ or (**B**) $CD4^+CD25^-Foxp3^+$ cells (Treg), isolated from *L. lactis*-based combination therapy (CT)-treated NOD.Foxp3.hCD2 mice (both responders and non-responders), and indicated neutralizing antibodies (10 µg/ml). Statistical significance between groups was calculated using Kruskal-Wallis test followed by Dunnett´s multiple testing; * $P < 0.05$, ** $P < 0.01$, *** $P < 0.001$. (**C**) *L. lactis*-based combination therapy-cured mice were injected with anti-CTLA4 and anti-TGF-β antibodies (n=5) and followed up for diabetes recurrence (mice with glucosuria and blood glucose measurements >200 mg/dl are represented by the dark circles).

Figure 6 – Specific inhibition of Treg function impairs therapy-induced tolerance. (**A**) Treatment scheme for the simultaneous administration of *L. lactis*-based combination therapy (CT) and the specific FOXP3 inhibitor P60 (i.p. 50 µg/daily) in new-onset diabetic NOD mice. (**B**) Shown is the

percentage of mice that remained diabetic after treatment. In the Kaplan-Meier survival curve, statistical significance between groups was determined by Mantel-Cox log-rank test; * $P < 0.05$.

Figure 7 – Foxp3$^+$ T cell depletion breaches *L. lactis*-based combination therapy-induced tolerance in NOD.Foxp3.DTR mice. (**A**) Treatment scheme for Foxp3$^+$ T cell depletion by DT in *L. lactis*-based combination therapy (CT)-cured NOD.Foxp3.DTR mice. (**B**) Blood glucose measurements in new-onset diabetic NOD.Foxp3.DTR mice during *L. lactis*-based combination therapy (n=7) and after DT treatment (n=4). Mice were considered cured (white symbols) when random blood glucose concentrations recovered to beneath 200 mg/dl or non-cured (black symbols) when mice sustained blood glucose concentrations above 200 mg/dl. (**C**) Insulitis scoring and (**D**) quantification of islet-resident Foxp3$^+$ T cells in the pancreas of therapy-cured NOD.Foxp3.DTR mice before and after DT treatement. Staining of representative pancreas section from a combination therapy-tolerized mice for CD4 (red) and Foxp3 (green) in which the white arrow heads indicate the presence of Foxp3$^+$ T cells within an islet of Langerhans. Statistical significance was calculated using Mann-Whitney t-test; ****, $P < 0.0001$.

Supplemental figure legends

Supplemental Figure S1 – *L. lactis*-based combination therapy induces higher percentage of CTLA4$^+$ Tregs in the pancreas of responder mice. The percentages of CTLA4$^+$ cells within the CD4$^+$CD25$^+$Foxp3$^+$ (left), CD4$^+$CD25$^-$Foxp3$^+$ (middle), and CD4$^+$Foxp3$^+$ (right) T cell population in peripheral blood (**A**), pancreatic draining lymph nodes (**B**) and pancreas (**C**) of new-onset diabetic and *L. lactis*-based combination therapy (CT)-treated mice (both responders and non-responders). Each symbol represents one mouse, and horizontal bars indicate the median value. Statistical significance was calculated using Mann-Whitney t-test; * $P < 0.05$, ** $P < 0.01$, ***, $P < 0.001$; ****, $P < 0.0001$.

Supplemental Figure S2 – *L. lactis*-based combination therapy-tolerized mice are not depleted in pathogenic T effector cells. Adoptive transfer of total splenocytes (1×10^7) isolated from overtly diabetic (white diamonds), combination therapy (CT) responders (white circles) or non-responders (crossed circles). Statistical calculation was done using Mantel-Cox log-rank test, ns: not significant.

Supplemental Figure S3 – Depletion of Foxp3$^+$ cells with DT in unmanipulated NOD.Foxp3.DTR mice. After four consecutive i.p. DT injections (on day (d) 1, 2, 5 and 7)(40 µg/kg body weight/d) as indicated in the scheme (**A**), mice (n=6) were killed on day 8, and peripheral blood and pancreas were removed. (**B**) Flow cytometric analysis of peripheral blood demonstrated efficient depletion of Foxp3$^+$ cells in DT-treated NOD.Foxp3.DTR mice. Foxp3 staining of pancreas sections showed effective depletion of islet-resident Foxp3$^+$ cells in DT-treated NOD.Foxp3.DTR mice. (**C**) Representative flow cytometric profiles showing the percentage of CD4$^+$ T cells positive for Foxp3 and the DTR-GFP fusion protein before (d0) and after two consecutive DT injections (d3 and 5) of NOD.Foxp3.DTR mice (left panel). (**D**) Rapid diabetes onset upon acute Foxp3$^+$ Treg depletion in NOD.Foxp3.DTR mice.

Supplemental Research Design and Methods

Construction of clinical-grade self-containing L. lactis secreting human PINS and IL10.

sAGX0407, engineered to secrete human PINS along with human IL10 (secreting 1.75 ng/ml PINS; 17.5 ng/ml IL10) was generated by replacement of the chromosomally-located thymidylate synthase (thyA) gene in an MG1363 parental strain by an expression cassette for human PINS and IL10 as described (1; 2). In brief, the method to introduce changes in the *L. lactis* chromosome makes use of double homologous recombination. A conditionally replicative carrier plasmid derived from pORI19 and containing an erythromycin selection marker, was constructed in the repA+ *L. lactis* strain LL108. Carrier plasmids are designed in such way that the cargo of interest is cloned in between up to 1 kb cross over (XO) areas, identical to the ones flanking the wild type sequence on the bacterial chromosome. This plasmid is introduced in MG1363 or any of its derivatives (repA-), resistant colonies are selected on agar plates containing erythromycin and a first homologous recombination either at the 5' or 3' target sites is verified by PCR screening. Release of erythromycin selection will enable the excision of the carrier plasmid from the bacterial chromosome by a second homologous recombination, at either the 5' or 3' target site. The final genetic structure of the clinical-grade strain is extensively documented by both Sanger and Illumina full genome sequencing. There are no plasmids or residual erythromycin resistance in the final clinical strain.

Bacteria and media.

The *L. lactis*-pT1NX is an MG1363 strain containing the empty vector pT1NX, and served as control. The plasmid-driven *L. lactis* strain (sAGX0328 secreting plasmid-encoded human PINS (4.25 ng/ml) and chromosomally-integrated IL10 (32.5 ng/ml)) was cultured as described (3). As growth and survival of thyA-deficient *L. lactis* strains depends on the presence of thymidine in the growth medium, the clinical-grade *L. lactis* (secreting chromosomally-integrated human PINS and IL10) was cultured

in GM17T, i.e. M17 broth (BD, Franklin Lakes, NJ), supplemented with 0.5% glucose (Merck KGaA, Darmstadt, Germany) and 200 µM thymidine (Sigma, St. Louis, MO). For intragastric inoculations, stock suspensions were diluted 1000-fold in growth media and incubated for 16 hours at 30°C, reaching a saturation density of 2×10^9 cfu/ml. Bacteria were harvested by centrifugation and concentrated 10-fold in BM9 medium. Treatment doses consisted of 100 µl of this bacterial suspension.

Flow cytometry.

Peripheral blood and specified organs were harvested 6 weeks after treatment initiation, processed and incubated with fluorochrome-labeled antibodies or matching isotype controls for flow cytometric analysis. Tregs were stained with anti-mouse CD3 (145-2C11), CD4 (GK1.5), CD8a (53-6.7), CD25 (PC61.5 or 7D4 (BD, Erembodegem, Belgium)), and FR4 (eBio12A5) (all from eBioscience, San Diego, CA, unless specified) for 20 min on ice. Intracellular staining antibodies against Foxp3 (FJK-16s) and CTLA4 (UC10-4B9) were from eBioscience and used according to the manufacturer's instructions. Naïve, effector memory and central memory T cells were determined by staining with anti-mouse CD3 (145-2C11), CD4 (GK1.5), CD8a (53-6.7), CD44 (IM7), CD62L (MEL-14), CD69 (H1.2F3), and CCR7 (4B12). Cells were analyzed in a Gallios™ flow cytometer with Kaluza (Beckman Coulter, Suarlée, Belgium) or FlowJo software (Treestar, Ashland, OR).

In vitro suppressor assays.

Pathogenic $CD4^+CD25^-$ Teff cells were isolated from spleen cells of 10-week old NOD mice by negative selection using antibodies to CD25, CD8α, B220, CD11c, CD11b, MHC class II, and sheep anti-rat IgG Dynabeads (Invitrogen, Merelbeke, Belgium). $CD4^+CD25^+Foxp3^+$ and $CD4^+CD25^-Foxp3^+$ Tregs were isolated from pooled lymph node and spleen cells of NOD.Foxp3.hCD2 mice (harboring a human CD2-CD52 fusion protein, along with an intra-ribosomal

entry site, into the 3′ untranslated region of the endogenous foxp3 locus)(4). Briefly, cell samples were passed through a 70-µm cell strainer and suspended in RPMI1640 medium, centrifuged for 5 min at 1,500 rpm and suspended in RPMI1640 medium. The resultant cell suspension was counted, washed and first depleted of $CD8\alpha^+$, $B220^+$, $CD11c^+$, $CD11b^+$ and MHC $class^+$, and adherent cells by panning and stained with biotin-conjugated anti-CD4 and anti-hCD2 antibodies. Cells were then incubated with anti-biotin microbeads ((Miltenyi Biotec B.V., Leiden, The Netherlands) and separated on LS or MS columns (Miltenyi Biotech). The resulting $hCD2^+$ or $hCD2^-$ cells were further purified with anti-CD25 antibodies. *In vitro* polyclonal suppressor assays were conducted as described (3). Cytokines (IFN-γ, IL10 and TGF-β) were measured in cell-free supernatants by multiplex immunoassay (Mesoscale Discovery, Rockville, MA) or flow cytometric bead array (Bender MedSystems FlowCytomix™, eBioscience) as described (3).

In additional set of experiments, blocking antibodies against CTLA4 (UC10-4F10; kind gift of Dr. Boon, Bioceros BV, Utrecht, The Netherlands), IL10 (clone JES5-2A5, BioXCell), and TGF-β (clone 1D11.16.8, which neutralizes all three mammalian TGF-β isoforms (β1, β2, and β3), BioXCell) were added to cultures at concentration of 10 µg/ml.

References

1. Steidler L, Neirynck S, Huyghebaert N, Snoeck V, Vermeire A, Goddeeris B, Cox E, Remon JP, Remaut E: Biological containment of genetically modified Lactococcus lactis for intestinal delivery of human interleukin 10. Nat Biotechnol 2003;21:785-789

2. Steidler L, Rottiers P: Therapeutic drug delivery by genetically modified Lactococcus lactis. Annals of the New York Academy of Sciences 2006;1072:176-186

3. Takiishi T, Korf H, Van Belle TL, Robert S, Grieco FA, Caluwaerts S, Galleri L, Spagnuolo I, Steidler L, Van Huynegem K, Demetter P, Wasserfall C, Atkinson MA, Dotta F, Rottiers P, Gysemans C, Mathieu C: Reversal of autoimmune diabetes by restoration of antigen-specific tolerance using genetically modified Lactococcus lactis in mice. J Clin Invest 2012;122:1717-1725

4. Kendal AR, Chen Y, Regateiro FS, Ma J, Adams E, Cobbold SP, Hori S, Waldmann H: Sustained suppression by Foxp3+ regulatory T cells is vital for infectious transplantation tolerance. The Journal of experimental medicine 2011;208:2043-2053

A

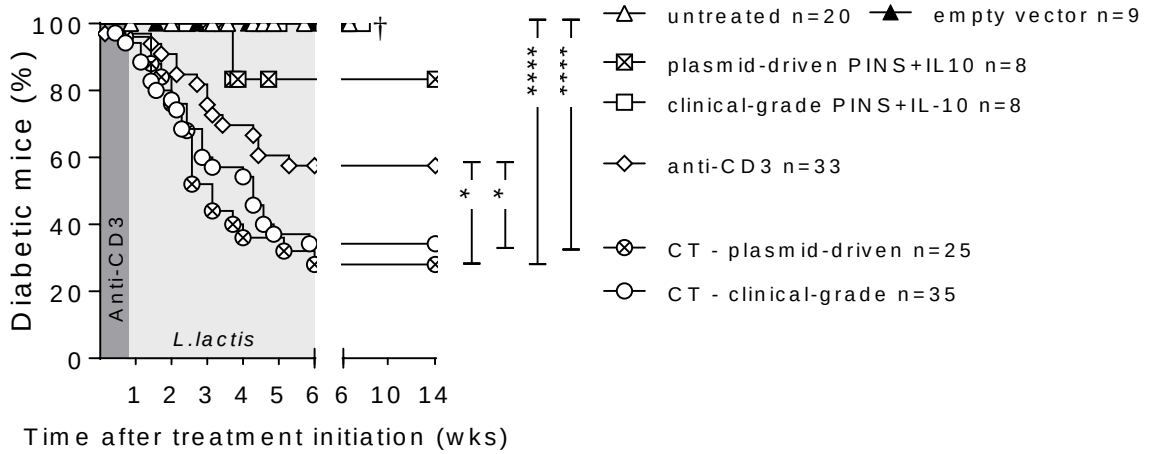
Diabetic mice (%)
100
80
60
40
20
0
Anti-CD3
L.lactis
1 2 3 4 5 6 6 10 14
Time after treatment initiation (wks)
†
*
*
****
****
untreated n=20
empty vector n=9
plasmid-driven PINS+IL10 n=8
clinical-grade PINS+IL-10 n=8
anti-CD3 n=33
CT - plasmid-driven n=25
CT - clinical-grade n=35

B

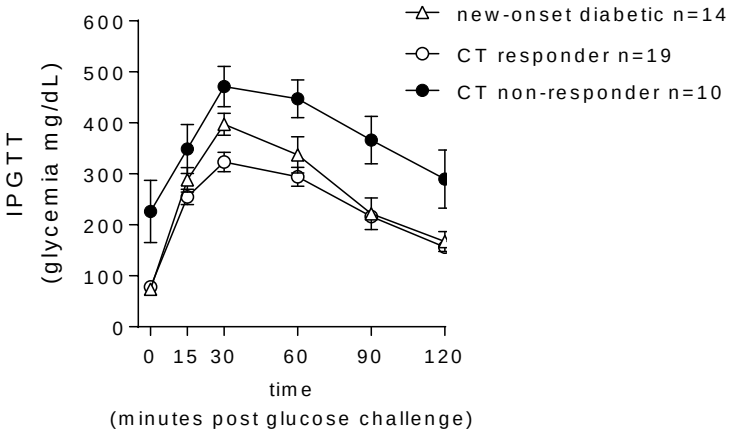
IPGTT
(glycemia mg/dL)
600
500
400
300
200
100
0
0 15 30 60 90 120
time
(minutes post glucose challenge)
new-onset diabetic n=14
CT responder n=19
CT non-responder n=10

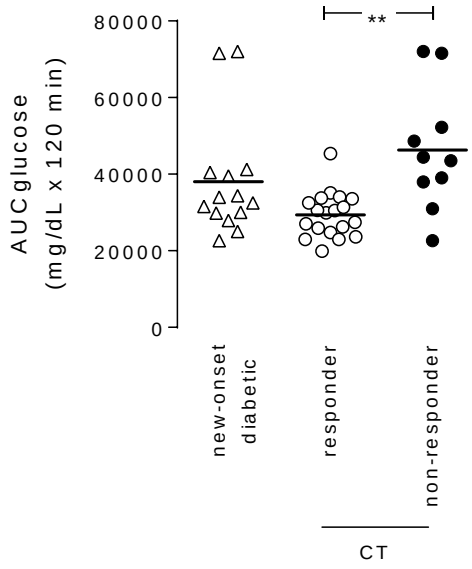
AUCglucose
(mg/dL x 120 min)
80000
60000
40000
20000
0
**
new-onset diabetic
responder
non-responder
CT

C

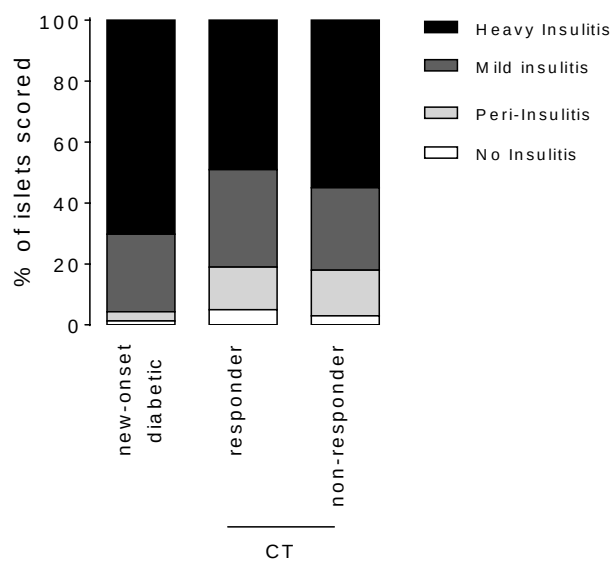
% of islets scored
100
80
60
40
20
0
new-onset diabetic
responder
non-responder
CT
Heavy Insulitis
Mild insulitis
Peri-Insulitis
No Insulitis

Figure 2

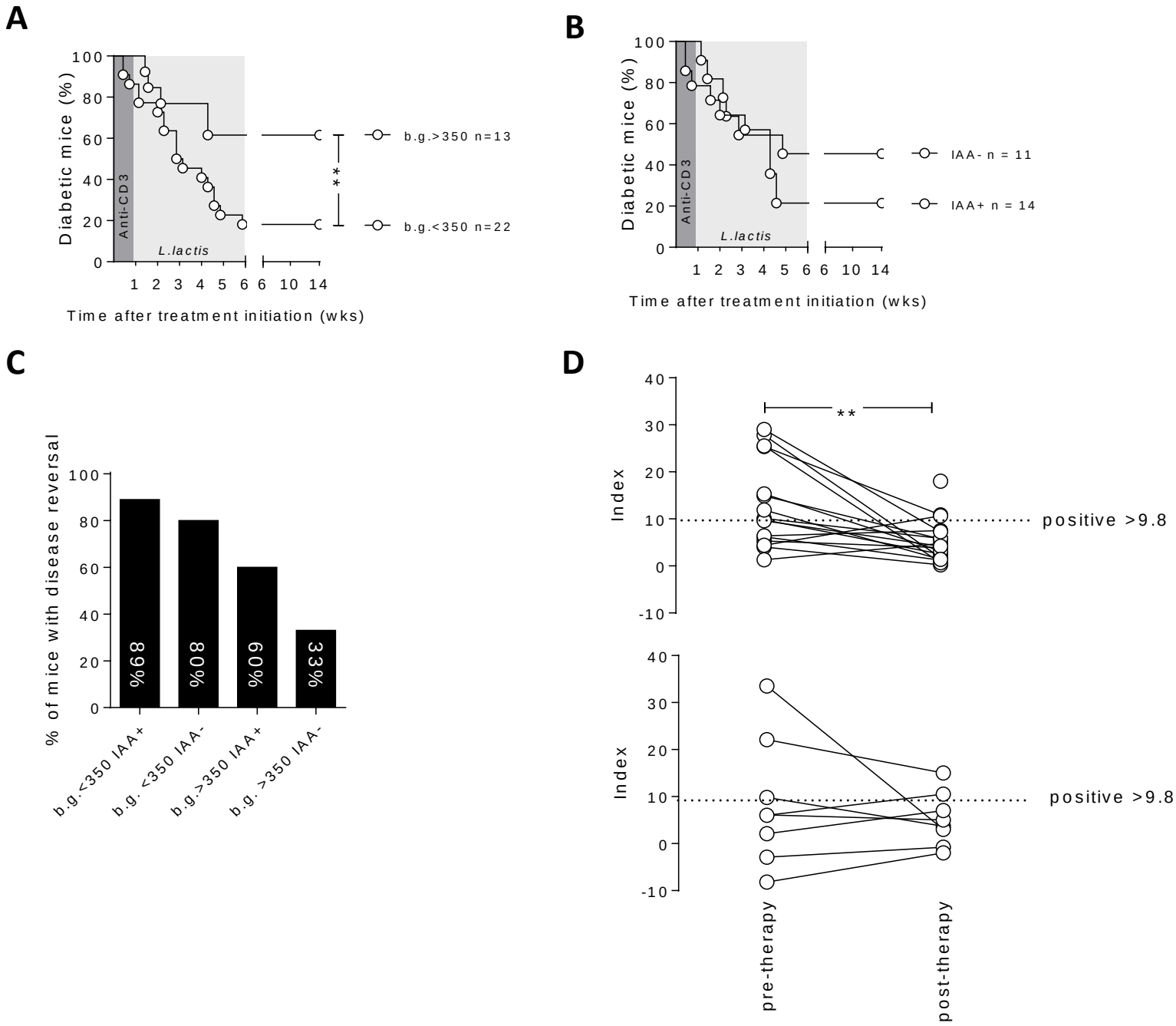
A
Diabetic mice (%)
Anti-CD3
L.lactis
b.g.>350 n=13
b.g.<350 n=22
**
Time after treatment initiation (wks)
B
Diabetic mice (%)
Anti-CD3
L.lactis
IAA- n = 11
IAA+ n = 14
Time after treatment initiation (wks)
C
% of mice with disease reversal
%68
%08
%09
%33
b.g.<350 IAA+
b.g. <350 IAA-
b.g.>350 IAA+
b.g. >350 IAA-
D
Index
**
positive >9.8
Index
positive >9.8
pre-therapy
post-therapy

Figure 3

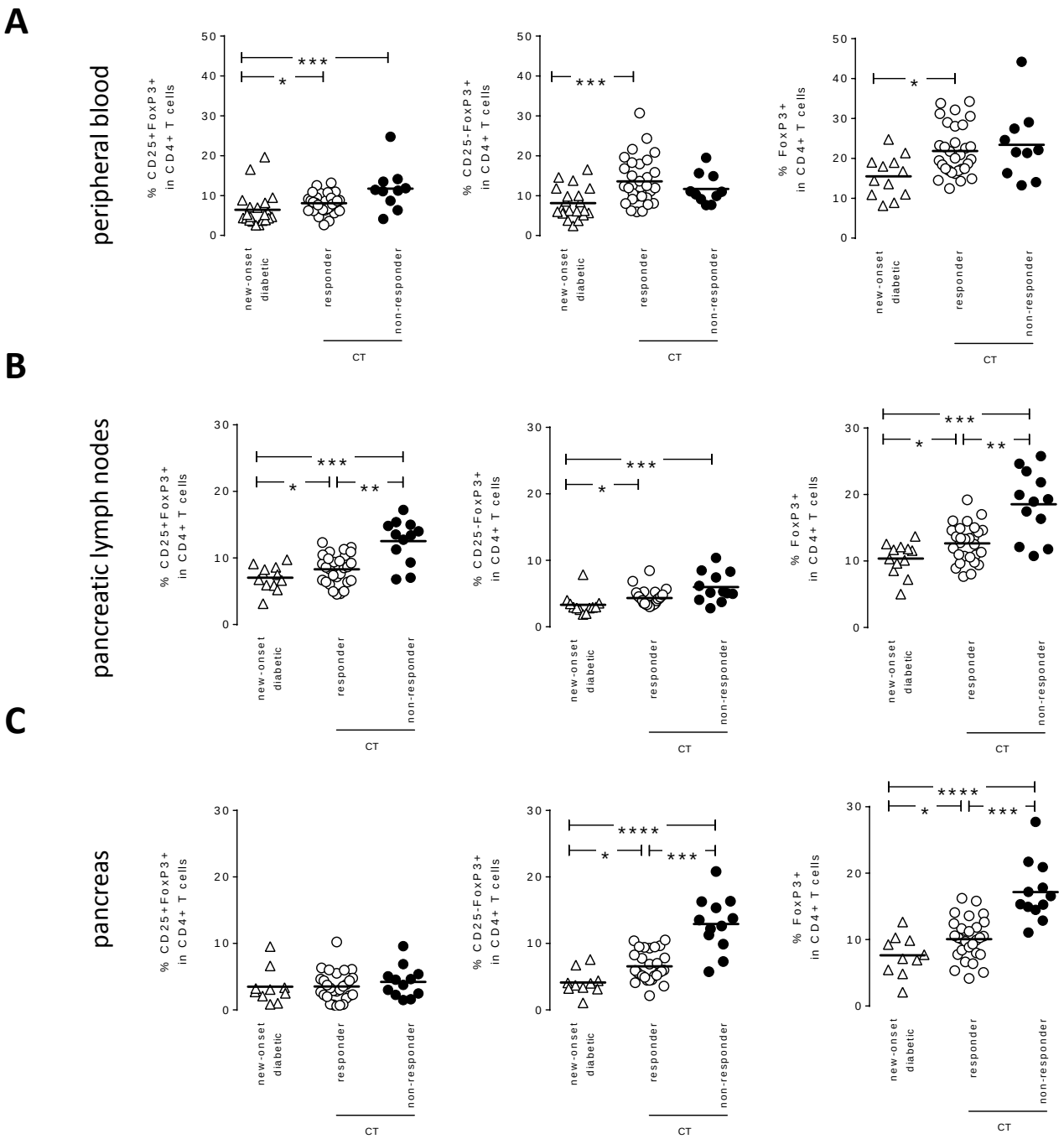
A
peripheral blood
B
pancreatic lymph nodes
C
pancreas
% CD25+FoxP3+ in CD4+ T cells
% CD25-FoxP3+ in CD4+ T cells
% FoxP3+ in CD4+ T cells
new-onset diabetic
responder
non-responder
CT

Figure 3

D
peripheral blood
% CD25+Foxp3+CTLA4+ in CD4+ T cells
% CD25-FoxP3+CTLA4+ in CD4+ T cells
% Foxp3+CTLA4+ in CD4+ T cells
new-onset diabetic
responder
non-responder
CT
E
pancreatic lymph nodes
% CD25+FoxP3+CTLA4+ in CD4+ T cells
% CD25-FoxP3+CTLA4+ in CD4+ T cells
% FoxP3+CTLA4+ in CD4+ T cells
F
pancreas
% CD25+FoxP3+CTLA4+ in CD4+ T cells
% CD25-FoxP3+CTLA4+ in CD4+ T cells
% FoxP3+CTLA4+ in CD4+ T cells

Figure 4

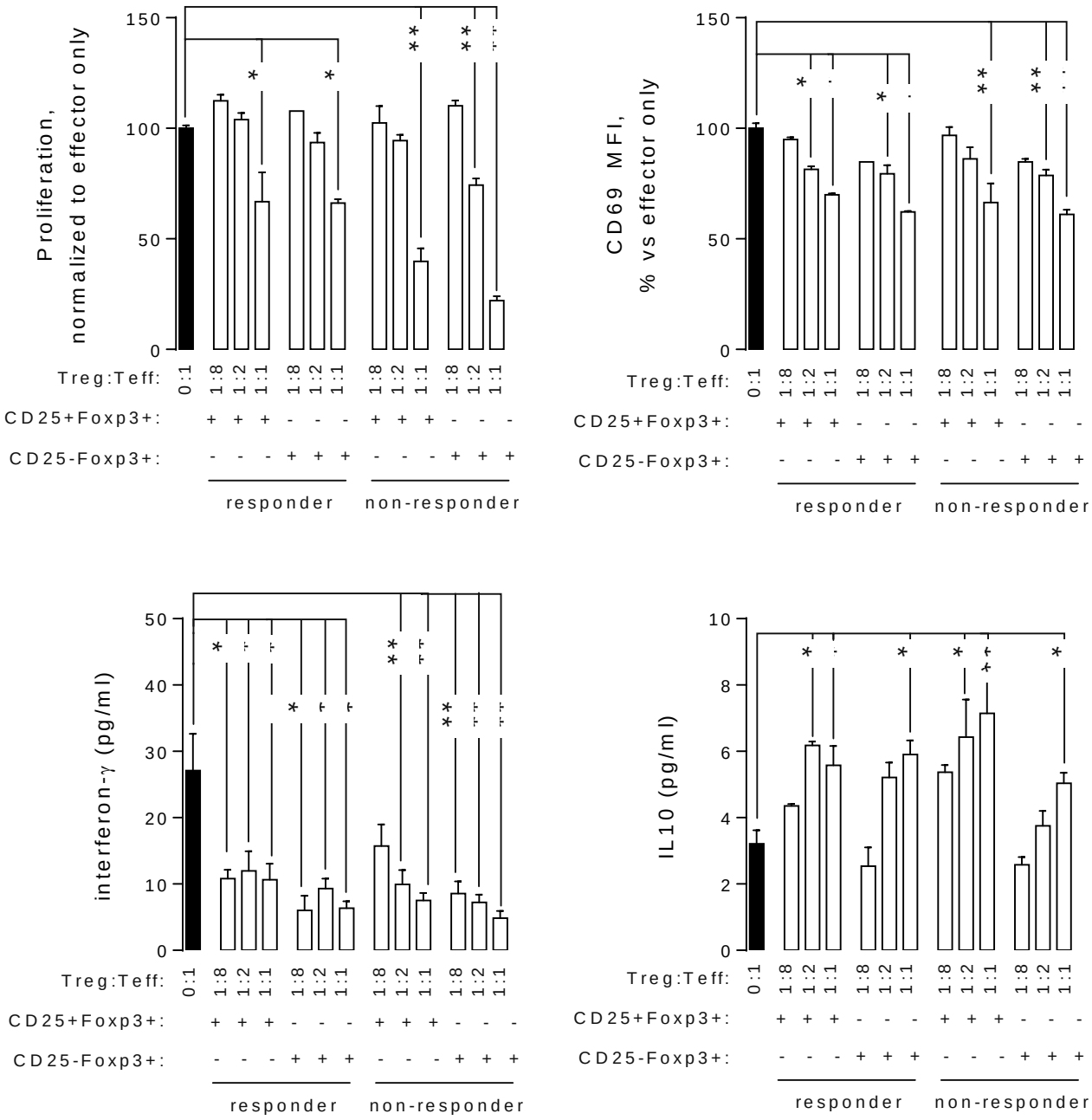
Proliferation, normalized to effector only
CD69 MFI, % vs effector only
interferon-γ (pg/ml)
IL10 (pg/ml)
Treg:Teff:
0:1
1:8
1:2
1:1
CD25+Foxp3+:
CD25-Foxp3+:
responder
non-responder

Figure 5

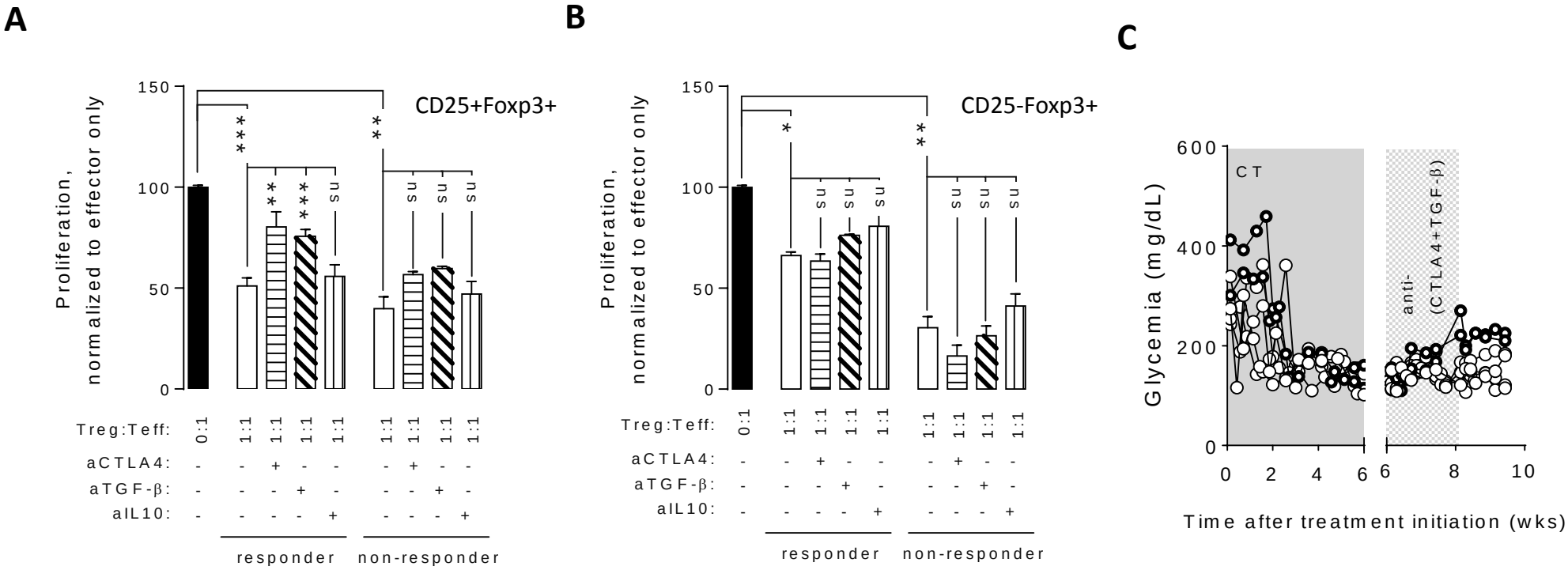
A
CD25+Foxp3+
Proliferation, normalized to effector only
150
100
50
0
***
**
***
**
su
Treg:Teff:
0:1
1:1
aCTLA4:
aTGF-β:
aIL10:
responder
non-responder
B
CD25-Foxp3+
*
**
C
Glycemia (mg/dL)
600
400
200
0
CT
anti-(CTLA4+TGF-β)
0
2
4
6
8
10
Time after treatment initiation (wks)

A

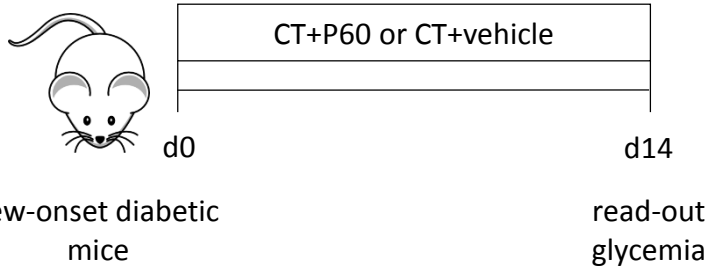
CT+P60 or CT+vehicle
d0
d14
new-onset diabetic mice
read-out glycemia

B

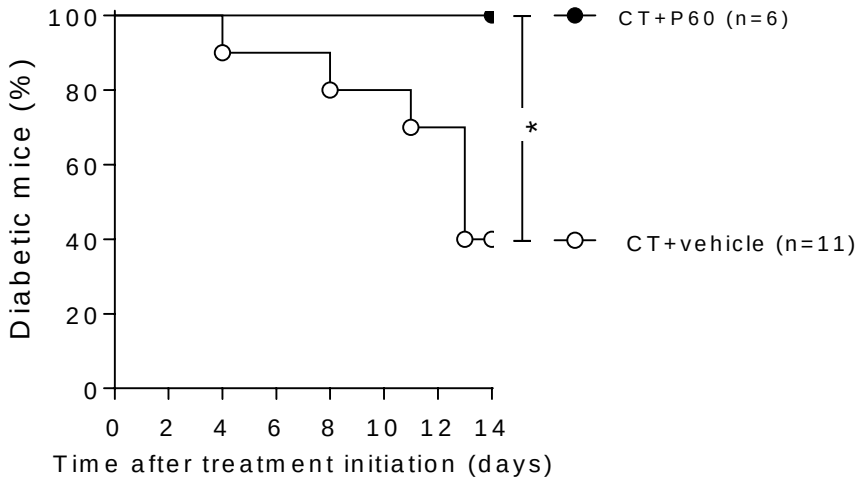
Diabetic mice (%)
100
80
60
40
20
0
0 2 4 6 8 10 12 14
Time after treatment initiation (days)
CT+P60 (n=6)
CT+vehicle (n=11)
*

Figure 7

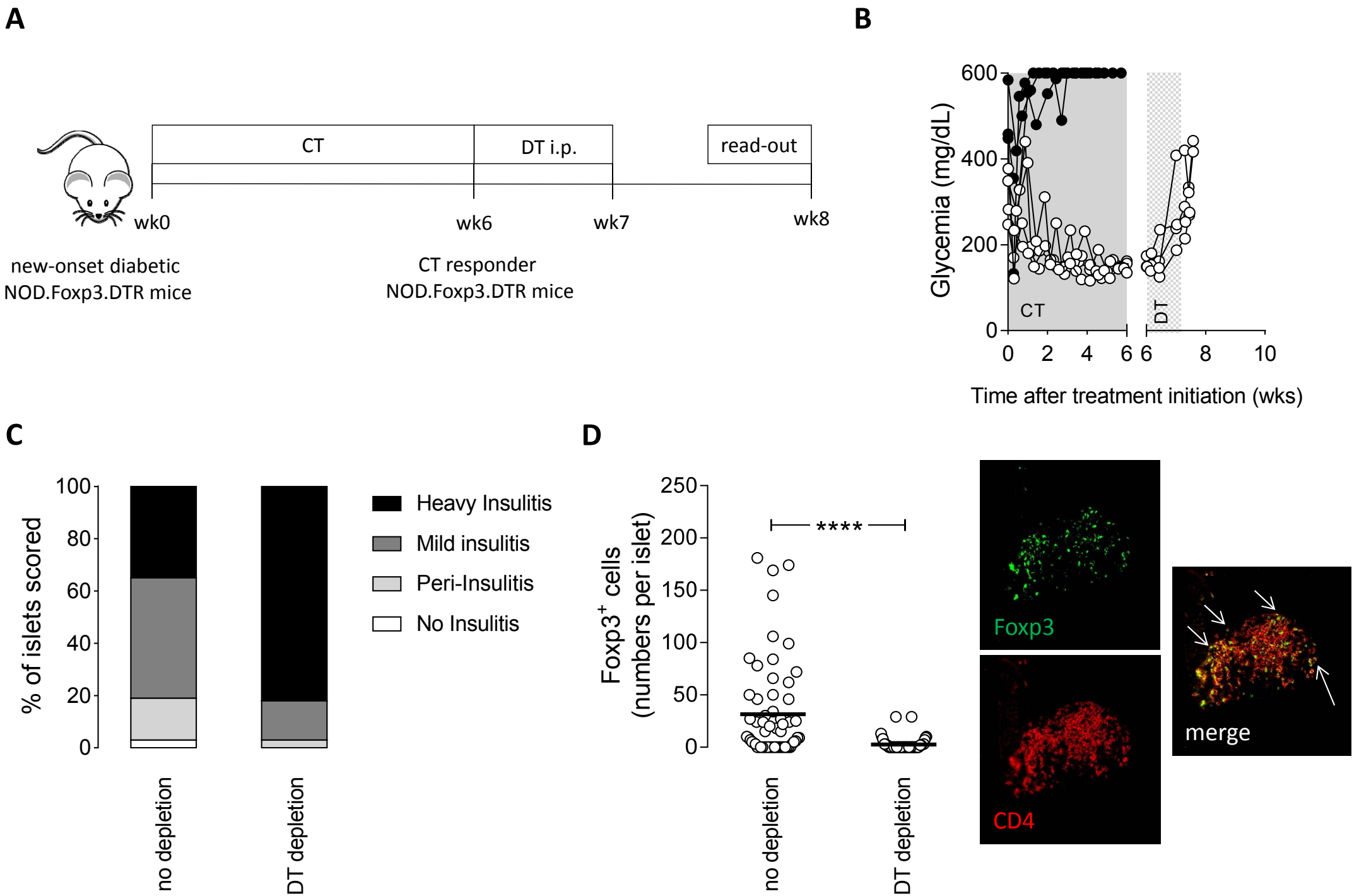
A
CT
DT i.p.
read-out
wk0
wk6
wk7
wk8
new-onset diabetic
NOD.Foxp3.DTR mice
CT responder
NOD.Foxp3.DTR mice
B
Glycemia (mg/dL)
600
400
200
0
CT
DT
0
2
4
6
6
8
10
Time after treatment initiation (wks)
C
% of islets scored
100
80
60
40
20
0
Heavy Insulitis
Mild insulitis
Peri-Insulitis
No Insulitis
no depletion
DT depletion
D
Foxp3+ cells
(numbers per islet)
250
200
150
100
50
0
****
no depletion
DT depletion
Foxp3
CD4
merge

Supplementary Figure 1

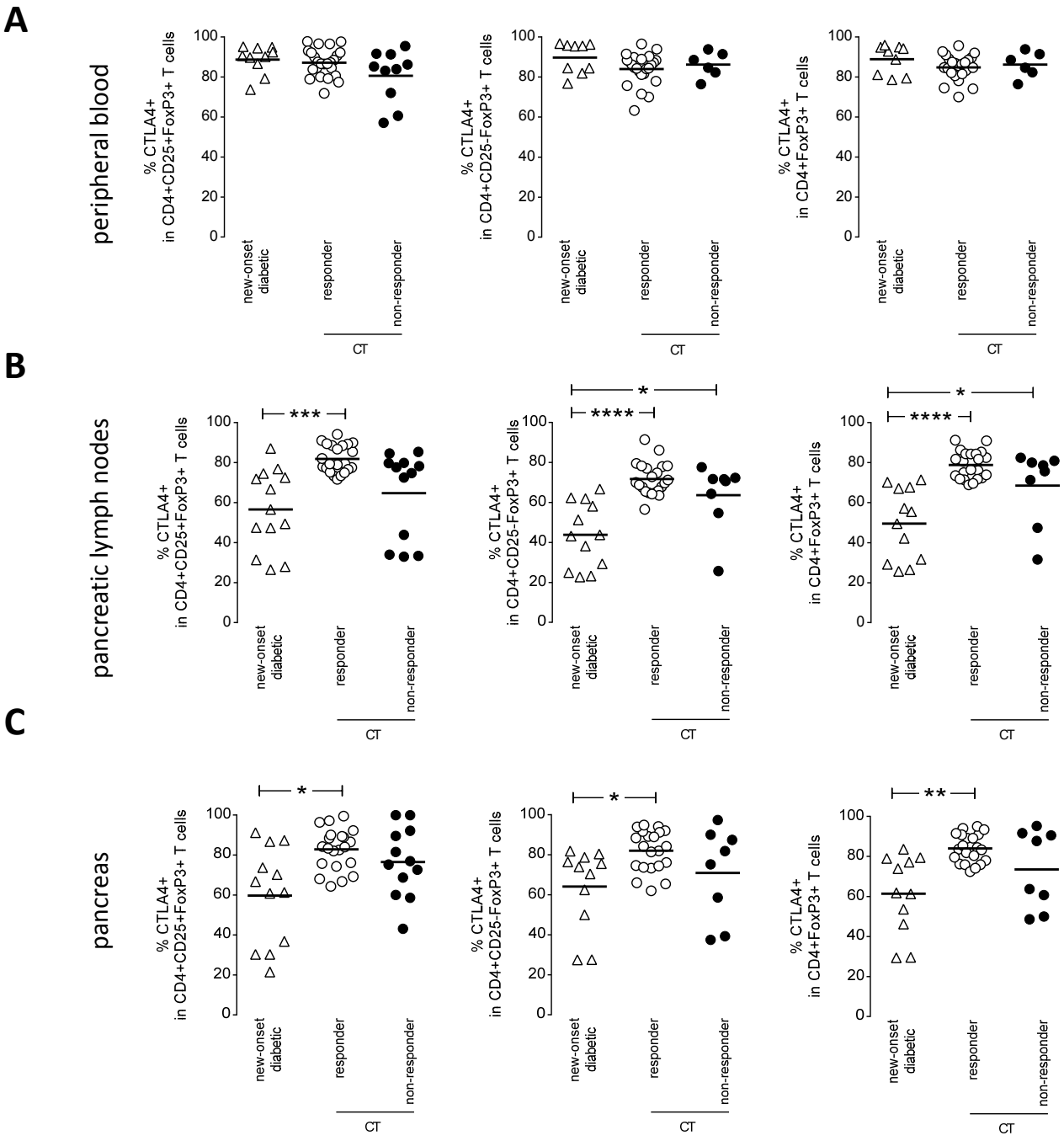

Supplementary Figure 2

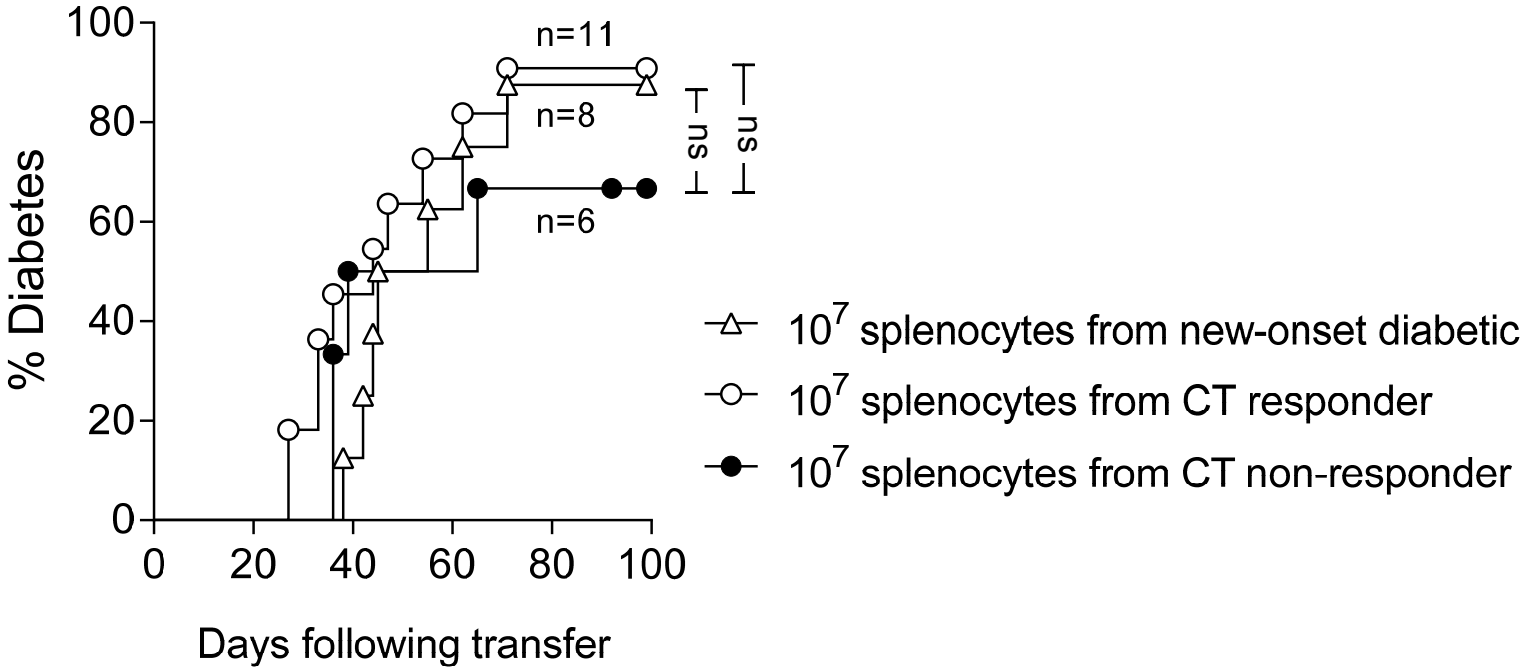

Supplementary Figure 3